

# Thermochemical and kinetic investigations of amorphous silica dissolution in NaOH solutions

Meriem Fertani-Gmati<sup>1</sup> · Mohamed Jemal<sup>1</sup>

Received: 9 June 2015 / Accepted: 8 August 2015 / Published online: 2 September 2015  
© Akadémiai Kiadó, Budapest, Hungary 2015

**Abstract** Dissolution of amorphous silica in 4, 8 and 11 mass% of sodium hydroxide solutions was followed by microcalorimetry at temperature between 353.15 and 403.15 K. Decreasing the Na<sub>2</sub>O/SiO<sub>2</sub> molar ratio leads to the successive formation of the following dissolved entities Si<sub>4</sub>O<sub>11</sub>Na<sub>6</sub>, Si<sub>2</sub>O<sub>5</sub>Na<sub>2</sub>, Si<sub>3</sub>O<sub>7</sub>Na<sub>2</sub> and Si<sub>5</sub>O<sub>11</sub>Na<sub>2</sub>. Their formation enthalpies were determined at 393.15 K as −5640.8, −2492.2, −3401.8 and −5214.7 kJ mol<sup>−1</sup>, respectively. A kinetic investigation showed that dissolution cannot be described by one-step controlled process. Isoconversional model allows determining a complex variation in the activation energy of dissolution in the range 6–21 kJ mol<sup>−1</sup>.

**Keywords** Calorimetry · Amorphous silica dissolution · Enthalpy of crystallization · Enthalpy of formation · Kinetics · Activation energy

## Introduction

Depending on the Na<sub>2</sub>O/SiO<sub>2</sub> molar ratio, soluble sodium silicates have many diversified industrial applications because of some features which are not shared by other alkaline solutions. Their chemical properties and functional characteristics, such as buffering capacity, surface charges modifying ability, polymerizing capability and high viscosity, can be utilized to solve many problems which arise

in chemical and industrial processes [1–5]. On the other hand, Karami and Rohani [6] used soluble sodium silicates for the synthesis of pure zeolite Y. Silicates have also been used for their effects in biology and particularly during their incorporation into collagen to regulate musculoskeletal tissue [7, 8].

In our previous works [9, 10], the experimental conditions which allow obtaining sodium silicate solutions have been determined and thermochemical and kinetic aspects of the  $\alpha$ -cristobalite dissolution in sodium hydroxide solutions have been studied. The process has been followed using a C-80 SETARAM calorimeter and led to the successive formation of dissolved entities whose formula depends on the Na<sub>2</sub>O/SiO<sub>2</sub> molar ratio.

It was interesting to determine how the thermochemical and kinetic parameters are modified when the silica variety changes. This paper deals with the dissolution of amorphous silica in NaOH solutions at different temperatures (353.15–403.15 K) and alkali concentrations.

## Experimental

As previously, dissolution of amorphous silica in an aqueous solution having 4, 8 and 11 mass% of NaOH (1.04, 2.17 and 3.08 mol L<sup>−1</sup>, respectively) has been carried out in isothermal conditions using a C-80 SETARAM microcalorimeter provided with a couple of hermetic cells. The lower compartment of the reaction cell was filled with the solid and tightly separated from the NaOH solution by a metallic cover. Beyond 80 mg, amorphous silica clogs and the dissolution stopped on the way. Consequently, the silica amount was fixed between 60 and 70 mg and the liquid volume was varied between 0.3 and 5 mL, so that the Na<sub>2</sub>O/SiO<sub>2</sub> molar ratio (*R*) ranges in 0.13–4.84 interval.

✉ Mohamed Jemal  
jemal@planet.tn

<sup>1</sup> Faculté des Sciences de Tunis, Chemistry Department, LR01SE10 Applied Thermodynamics Laboratory, Université de Tunis El Manar, 2092 Tunis, Tunisia

After one night of stabilization time at a constant temperature between 353.15 and 403.15 K, the reactants were mixed using the reversal mechanism system of the device and the dissolution was followed until equilibrium.

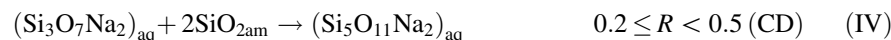
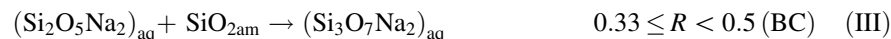
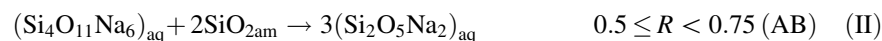
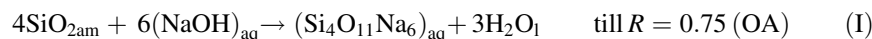
Table 1 summarizes relevant information on the provenance and purity of the starting materials.

The calorimeter has been checked with the key reaction by measuring the heat quantity resulting from dissolution of trihydroxymethylaminomethane (TRIS) in 5 mL of a 0.1 molal HCl solution. Dissolving increasing amounts of TRIS led to a linear expression of the heat quantity as a function of TRIS mass, the slope of which gave the molar enthalpy as  $-30.14 \pm 0.27 \text{ kJ mol}^{-1}$ . This value differs from those of the literature ( $-29.7447$  [11],  $-29.773$  [12] and  $-29.765 \text{ kJ mol}^{-1}$  [13]) by no more than 1.2 %.

## Results and discussion

### Dissolution thermochemistry

The heat amount corresponding to dissolution of various amounts of amorphous silica in 1 g of NaOH solution was



calculated from the global energy determined by integrating the rough signal (Table 2). The drawing of the absolute value of this quantity over the solid mole number shows five segments, OA, AB, BC, CD and DE, successively corresponding to different domains (Fig. 1).

Least-square processing led to OA an equation in the form  $y = ax + b$ , where  $b$  has been assigned to the reversing mechanical operation. However, a statistical treatment [14] allowed concluding that the intercept was statistically insignificant. Consequently, the OA equation has been expressed as  $-Q_{\text{mes}} = 15.64n_{\text{SiO}_2}$ .

It should be noticed that dissolution of  $\alpha$ -cristobalite reported in the previous paper [9] has a similar beginning shape but has been stopped at the end of the third domain (BC) because the process became very slow when the

$\text{Na}_2\text{O}/\text{SiO}_2$  molar ratio decreases, needing in some cases a 4-day equilibrium time.

When the energy calculated for a constant amount of one of the reactants varies linearly in a certain domain, over the amount of the other reactant, this indicates that the same amount of energy per unit mole of the latter is involved (constant derivative), i.e., the same phenomenon occurs up to the end of the line. At this point, the reactants are at stoichiometric proportions, and so, the formula of the compound appearing along all the line composition range can be determined from the abscissa. As the upper points of lines in Fig. 1 appear at the  $\text{Na}_2\text{O}/\text{SiO}_2$  molar ratio values close to 0.75, 0.5, 0.33 and 0.2, the progressive dissolution of silica in these conditions led to the formation of dissolved  $\text{Si}_4\text{O}_{11}\text{Na}_6$ ,  $\text{Si}_2\text{O}_5\text{Na}_2$ ,  $\text{Si}_3\text{O}_7\text{Na}_2$  and  $\text{Si}_5\text{O}_{11}\text{Na}_2$  successively. The final horizontal line corresponds to equilibria between the latter in solution and undissolved silica which has been detected over  $2.94 \cdot 10^{-3} \text{ mol}$  in Fig. 1. No solid was observed after reaction in the preceding domains.

So, the four first domains in Fig. 1 correspond to the following reactions:

Enthalpies of these reactions at 393.15 K are calculated from the slopes of the corresponding segments drawn in Fig. 1. As the slopes refer to one silica mole, these enthalpies were calculated by the product of the slope of the line in a certain domain times the mole number of silica involved in the corresponding reaction. So, these quantities equal four, two, one and two times the slopes of their corresponding segment equations, respectively (Table 3).

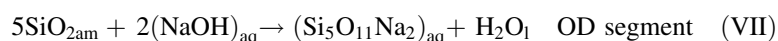
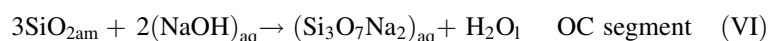
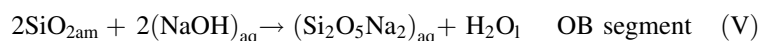
### Enthalpies of “one step” reactions

Figure 1 shows that except for the tetramer, dissolution leading to a certain oligomer occurs through the formation of one (or more) previous one(s). The dashed line joining

**Table 1** Chemicals used in this work

Compound	Source	Initial mole fraction purity
SiO <sub>2am</sub>	Fluka	High purity grade
NaOH	Chemi-Pharma	99 %

the origin (O) to a particular point (B, C or D) corresponds to a “one step” reaction between SiO<sub>2</sub> and NaOH solution leading to the corresponding oligomer. For the sake of clarity, only two dashed lines are represented on Fig. 1. These “one step” reactions are as follows:



Their molar enthalpies equal two, three or five times the slope of the corresponding dashed lines. Table 4 gathers the slopes of these lines together with the corresponding enthalpies.

### Thermochemical cycle

As (Si<sub>2</sub>O<sub>5</sub>Na<sub>2</sub>)<sub>aq</sub> can be obtained according to two paths (reactions II and V), it was interesting to check the coherence of the results considering the thermochemical cycle involving the tetrameric and dimeric forms (Fig. 2).

The first reaction corresponds to the “one step” path leading to three moles of dimer and involves six moles of silica, and its molar enthalpy ( $\Delta_R H_1$ ) equals six times the slope of the corresponding dashed line ( $-88.98 \text{ kJ mol}^{-1}$ ). The second one corresponds to the dissolution leading to

the tetramer ( $\Delta_R H_2 = -62.56 \text{ kJ mol}^{-1}$ ) and the third one to the transformation of the latter into dimer involving two moles of silica ( $\Delta_R H_3 = -27.58 \text{ kJ mol}^{-1}$ ). The sum ( $\Delta_R H_2 + \Delta_R H_3$ ) differs from  $\Delta_R H_1$  by only 1.3 %. In the

**Table 2** Amorphous silica (AS) dissolution data in 4 mass% NaOH solution (sln) at 393.15 K

$m_{\text{AS}}/\text{mg}$	$m_{\text{sln}}/\text{g}$	$-Q_{\text{mes}}/\text{J}$	$n_{\text{AS}}/\text{mol g}^{-1} \text{NaOH}_{\text{sln}}$	$-Q_{\text{mes}}/\text{J g}^{-1} \text{NaOH}_{\text{sln}}$
32.52	5.24	7.46	1.03 <sup>E-4</sup>	1.43
65.92	5.24	15.23	2.10 <sup>E-4</sup>	2.91
62.05	2.60	15.39	3.97 <sup>E-4</sup>	5.91
60.10	2.13	16.34	4.70 <sup>E-4</sup>	7.67
61.85	1.75	16.69	5.89 <sup>E-4</sup>	9.54
70.26	1.77	17.93	6.60 <sup>E-4</sup>	10.12
60.53	1.33	15.41	7.57 <sup>E-4</sup>	11.58
70.48	1.42	17.40	8.24 <sup>E-4</sup>	12.22
63.58	1.04	15.69	1.02 <sup>E-3</sup>	15.13
59.68	0.88	14.07	1.13 <sup>E-3</sup>	16.05
70.23	0.94	15.50	1.24 <sup>E-3</sup>	16.46
70.90	0.85	14.96	1.39 <sup>E-3</sup>	17.62
70.44	0.78	14.08	1.50 <sup>E-3</sup>	18.02
70.40	0.71	13.17	1.64 <sup>E-3</sup>	18.46
70.24	0.66	12.35	1.78 <sup>E-3</sup>	18.78
70.58	0.60	11.61	1.95 <sup>E-3</sup>	19.23
69.96	0.54	10.35	2.17 <sup>E-3</sup>	19.25
70.56	0.47	9.42	2.51 <sup>E-3</sup>	20.12
70.37	0.40	7.83	2.95 <sup>E-3</sup>	19.70
70.43	0.35	7.03	3.32 <sup>E-3</sup>	19.92
70.06	0.30	6.14	3.88 <sup>E-3</sup>	20.44

**Fig. 1** Heat amount corresponding to 1 g of alkali solution as a function of the silica mole number (in 4 mass% NaOH solution at 393.15 K)

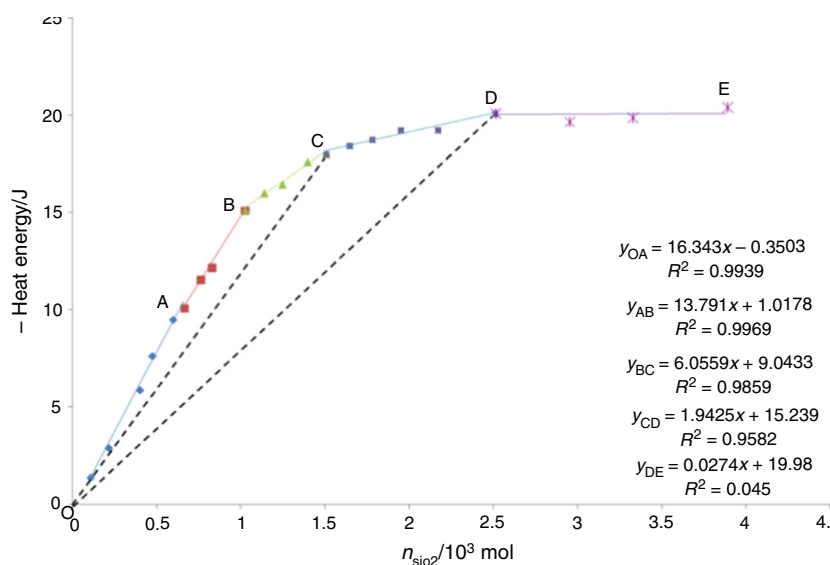


**Table 3** Line slopes and molar enthalpies of I–IV reactions in  $\text{kJ mol}^{-1}$  in 4 mass% NaOH solution

Domain	Line slope/ $\text{kJ mol}^{-1}$	$\Delta_{\text{sol}}H^a/\text{kJ mol}^{-1}$
OA	15.64	$-62.56 \pm 2.88$
AB	13.79	$-27.58 \pm 0.56$
BC	6.06	$-6.06 \pm 0.16$
CD	1.94	$-3.88 \pm 0.18$

<sup>a</sup> With expanded uncertainty  $U(\Delta_{\text{sol}}H)$  (level of confidence = 0.95)

case of  $\alpha$ -cristobalite, similar calculation gave a difference of 0.3 %. Other cycles involving the couples' dimer–trimer and trimer–pentamer gave a difference of 0.9 and 0.5 %, respectively. The coherence of these results confirms the assignment of the reactions to their corresponding domains.

Notice that it is possible to determine the enthalpy of direct transformation of an oligomer into any other one from the slope of the line joining the end points of their corresponding domain segments.

### Crystallization enthalpy

Taking into account the results previously obtained with  $\alpha$ -cristobalite, it is possible to determine the enthalpy of the

amorphous/ $\alpha$ -cristobalite transformation considering OA, OB and OC segments. Subtracting the couples of line slopes (continuous line for the tetramer and dashed ones for the dimer and trimer) leads to three values for the crystallization enthalpy at 393.15 K. Table 5 gathers the line slopes together with their differences (crystallization enthalpies).

So, the mean value at 393.15 K equals  $-3.23 \pm 0.39 \text{ kJ mol}^{-1}$ . The literature reported for this quantity values ranging between  $-2.51$  and  $-8.92 \text{ kJ mol}^{-1}$  [15] at temperature between 298 and 1999 K.

### Formation enthalpies of amorphous silica and various oligomers

Combining the crystallization enthalpy with the formation enthalpy of  $\alpha$ -cristobalite ( $-907.4 \pm 1.5 \text{ kJ mol}^{-1}$ ) [16] leads to  $(-904.2 \pm 1.6) \text{ kJ mol}^{-1}$  for the formation enthalpy of amorphous  $\text{SiO}_2$ . This value differs from those of the literature ( $-901.5$  [15] and  $-900.7 \text{ kJ mol}^{-1}$  [16]) by 0.4 and 0.3 %, respectively.

This quantity was combined with that of  $\text{H}_2\text{O}_l$  ( $-285.83 \pm 0.04 \text{ kJ mol}^{-1}$ ) [16] and that of  $(\text{NaOH}; 53.3 \text{ H}_2\text{O})_{\text{aq}}$  ( $-469.7 \text{ kJ mol}^{-1}$ ) [17] to give the formation

**Table 4** Dashed line slopes and molar enthalpies of “one step” reactions in 4 mass% NaOH solution

Segment	Entity	Dashed line slope/ $\text{kJ mol}^{-1}$	$\Delta_{\text{sol}}H^a/\text{kJ mol}^{-1}$
OB	$(\text{Si}_2\text{O}_5\text{Na}_2)_{\text{aq}}$	$-14.83$	$-29.66 \pm 0.56$
OC	$(\text{Si}_3\text{O}_7\text{Na}_2)_{\text{aq}}$	$-12.01$	$-36.03 \pm 0.48$
OD	$(\text{Si}_5\text{O}_{11}\text{Na}_2)_{\text{aq}}$	$-8.02$	$-40.1 \pm 0.45$

<sup>a</sup> With expanded uncertainty  $U(\Delta_{\text{sol}}H)$  (level of confidence = 0.95)

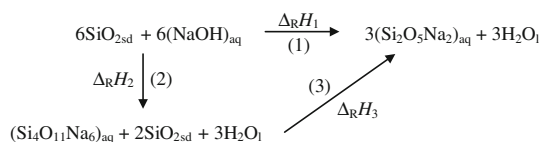


**Fig. 2** Thermochemical cycle of the transformation tetramer/dimer

enthalpy of  $(\text{Si}_4\text{O}_{11}\text{Na}_6)_{\text{aq}}$  as  $-5640.1 \text{ kJ mol}^{-1}$ , which differs from that determined from  $\alpha$ -cristobalite dissolution by only 0.03 %. The formation enthalpies of  $(\text{Si}_2\text{O}_5\text{Na}_2)_{\text{aq}}$ ,  $(\text{Si}_3\text{O}_7\text{Na}_2)_{\text{aq}}$  and  $(\text{Si}_5\text{O}_{11}\text{Na}_2)_{\text{aq}}$  can be determined from the successive transformation reactions (II), (III) and (IV) and from the “one step” hypothetical dissolution reactions (V), (VI) and (VII), respectively. Values are gathered in Table 6 together with those determined from  $\alpha$ -cristobalite dissolution. The difference between the extreme values in this table does not exceed 0.14 %.

Notice that all these calculations combine formation enthalpies at 298.15 K and 393.15 K, so they do not take into account their variation with respect to temperature according to Kirchhoff law.

The contribution to one  $\text{SiO}_2$  in the formation enthalpy increases as  $-1410.2$ ,  $-1246.1$ ,  $-1133.9$  and  $-1042.9 \text{ kJ mol}^{-1}$  in the  $(\text{Si}_4\text{O}_{11}\text{Na}_6)_{\text{aq}}$ ,  $(\text{Si}_2\text{O}_5\text{Na}_2)_{\text{aq}}$ ,  $(\text{Si}_3\text{O}_7\text{Na}_2)_{\text{aq}}$  and  $(\text{Si}_5\text{O}_{11}\text{Na}_2)_{\text{aq}}$  series, respectively, and so, the successive appearance of the oligomers is governed

by this quantity and not by the formation enthalpy. Neglecting the entropy factor, the lower the formation enthalpy per formular unit, the higher is the stability of the oligomer and so the earlier it appears.

On the other hand, it should be noticed that, in these compounds, the Na/Si atomic ratio is in the range 1.5–0.4, suggesting a cyclic structure. FTIR and  $^{29}\text{Si}$  NMR recordings performed on some of these compounds did not allow determining their structure.

### Dissolution kinetics in OA domain

For rapid reactions, kinetic study should be conducted on thermogenesis (or deconvoluted) curves. In the present work, these curves were obtained according to Brahim et al. procedure [18, 19] and showed exothermal effect for all the amounts of amorphous silica. Figure 3 highlights the difference between the crude (recorded) signal and the corresponding deconvoluted curve.

### Comparison with $\alpha$ -cristobalite behavior

Experiments were performed in 4 mass% NaOH solution at 393.15 K for a solid-to-liquid ratio (S/L) in the range of 0.62/100–3.96/100 g/g. The conversion rate was calculated by the ratio of the heat “ $q$ ” released until time “ $t$ ” over the

**Table 5** Couples of line slopes and crystallization enthalpy at 393.15 K

Segment	Entity	Line slope <sup>a</sup> /kJ mol <sup>-1</sup>		Crystallization enthalpy <sup>a</sup> $\Delta_{\text{cr}}H/\text{kJ mol}^{-1}$
		Amorphous silica	$\alpha$ -Cristobalite <sup>b</sup>	
OA	$(\text{Si}_4\text{O}_{11}\text{Na}_6)_{\text{aq}}$	$-15.64 \pm 0.72$	$-12.86 \pm 0.16$	$-2.82 \pm 0.74$
OB	$(\text{Si}_2\text{O}_5\text{Na}_2)_{\text{aq}}$	$-14.83 \pm 0.28$	$-11.27 \pm 0.07$	$-3.58 \pm 0.29$
OC	$(\text{Si}_3\text{O}_7\text{Na}_2)_{\text{aq}}$	$-12.01 \pm 0.16$	$-8.71 \pm 0.02$	$-3.31 \pm 0.16$

<sup>a</sup> With expanded uncertainty U (level of confidence = 0.95)

<sup>b</sup> Calculated from data in Ref. [9]

**Table 6** Formation enthalpies of various oligomers

	$\Delta_{\text{f}}H^{\circ}/\text{kJ mol}^{-1}$				Mean <sup>b</sup> /kJ mol <sup>-1</sup>
	Amorphous silica		$\alpha$ -Cristobalite <sup>c</sup>		
	Continuous line	Dashed line	Continuous line	Dashed line	
$(\text{Si}_4\text{O}_{11}\text{Na}_6)_{\text{aq}}$	$-5640.1 \pm 6.7^{\text{b}}$	–	$-5641.5 \pm 6.0^{\text{b}}$	–	$-5640.8 \pm 6.4$
$(\text{Si}_2\text{O}_5\text{Na}_2)_{\text{aq}}$	$-2492.0 \pm 2.5$	$-2491.6 \pm 3.0^{\text{b}}$	$-2490.9 \pm 2.3$	$-2494.4 \pm 3.2^{\text{b}}$	$-2492.2 \pm 2.8$
$(\text{Si}_3\text{O}_7\text{Na}_2)_{\text{aq}}$	$-3402.3 \pm 3.5$	$-3402.2 \pm 4.5^{\text{b}}$	$-3400.9 \pm 2.8$	$-3401.9 \pm 4.8^{\text{b}}$	$-3401.8 \pm 3.9$
$(\text{Si}_5\text{O}_{11}\text{Na}_2)_{\text{aq}}$	$-5214.6 \pm 4.6$	$-5214.7 \pm 7.6^{\text{b}}$	–	–	$-5214.7 \pm 6.1$

<sup>a</sup> With combined standard uncertainty  $U(\Delta_{\text{f}}H)$  (level of confidence = 0.95)

<sup>b</sup> Because of the lack of uncertainties on NaOH solution data in the literature, errors were calculated considering only the standard uncertainties of the other data

<sup>c</sup> Calculated from data in Ref. [9]

**Fig. 3** Example of raw (a) and deconvoluted (b) signals corresponding to the dissolution of 1.26 g of silica in 100 g of 4 mass% NaOH aqueous solution at 393.15 K

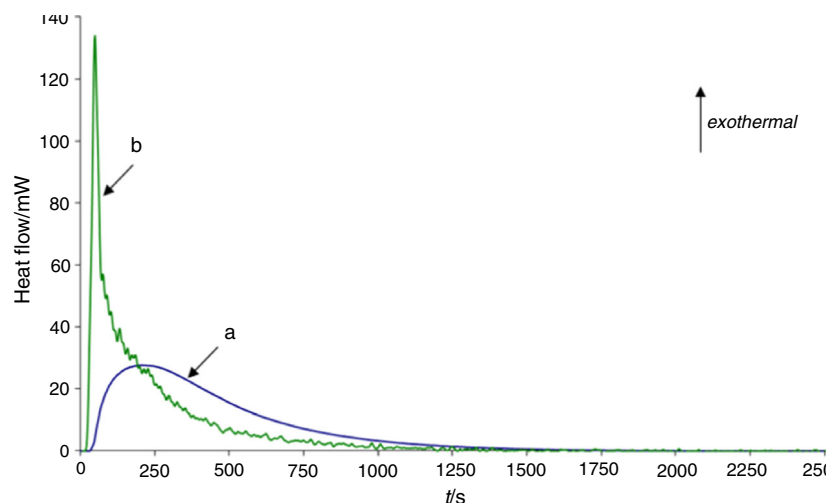


**Table 7** Amorphous silica (AS) dissolution data in 4 mass% NaOH solution (sln) at 353.15 to 403.15 K

$T/K$	$m_{AS}/mg$	$m_{sln}/g$	$-Q_{mes}/J$	$n_{AS}/mol\ g^{-1}\ NaOH_{sln}$	$-Q_{mes}/J\ g^{-1}\ NaOH_{sln}$
353.15	59.97	2.11	19.54	$4.73^{E-4}$	9.26
363.15	60.68	2.07	19.19	$4.88^{E-4}$	9.27
373.15	60.49	2.11	17.79	$4.77^{E-4}$	8.43
383.15	60.08	2.09	17.09	$4.78^{E-4}$	8.18
393.15	60.10	2.13	16.34	$4.70^{E-4}$	7.67
403.15	60.32	2.09	14.99	$4.80^{E-4}$	7.17

overall heat “ $Q$ ” corresponding to the whole dissolution process.

The dissolution conversion rate increases as the solid-to-liquid ratio increases for both  $\alpha$ -cristobalite and amorphous forms (not reported).

As with  $\alpha$ -cristobalite, some experiments were carried out on the amorphous form at different reaction temperatures in the range of 353.15–403.15 K for the same solid-to-liquid ratio ( $S/L = 2.9/100\ g/g$ ) and the same alkali concentration (4 mass% NaOH). The dissolution data are gathered in Table 7. It was observed (not reported) that the dissolution rate increases as the reaction temperature increases, except at 353.15 and 403.15 K for which the reaction rate is higher or lower than at all the other temperatures, respectively. These anomalies which did not appear with  $\alpha$ -cristobalite suggest the occurrence of different phenomena at these temperatures.

The effect of the alkali concentration on the conversion rate at 393.15 K was analyzed considering the three concentrations (4, 8 and 11 mass% NaOH) for the same solid-to-liquid ratio ( $S/L = 2.9/100\ g/g$ ), and the dissolution data are gathered in Table 8. Figure 4 shows the

conversion rate variations over time for different concentrations for both forms of silica. One can notice that there is not a regular variation for amorphous silica which confirms the complexity of its behavior.

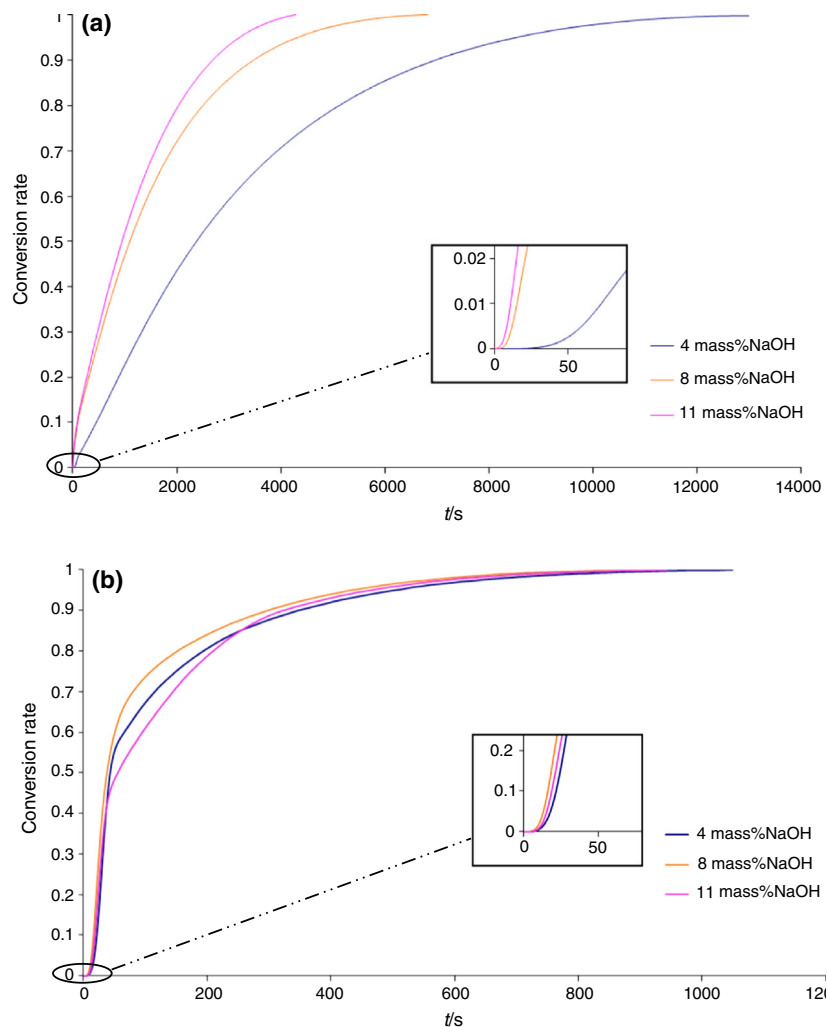
Moreover, Fig. 4 shows for both forms an initial phase of a few seconds corresponding to an induction period after which dissolution phenomenon starts. This latency time is particularly important for dissolution of  $\alpha$ -cristobalite in 4 mass% solution. Subtracting this time from the experimental results for amorphous form had no influence on the conclusions regarding the kinetic analysis by the shrinking core model (next section).

### Shrinking core model

The heterogeneous reaction models have been considered to determine the kinetic parameters and the rate-controlling step of the amorphous silica dissolution. The rate equations in these models have been widely developed in the literature [20–22] and are based on the following equation [23]:

**Table 8** Amorphous silica (AS) dissolution data in 4, 8 and 11 mass% NaOH solution (sln) at 393.15 K

mass% NaOH	$m_{AS}/\text{mg}$	$m_{sln}/\text{g}$	$-Q_{mes}/\text{J}$	$n_{AS}/\text{mol g}^{-1} \text{NaOH}_{sln}$	$-Q_{mes}/\text{J g}^{-1} \text{NaOH}_{sln}$
4	60.10	2.13	16.34	$4.70^E -4$	7.67
8	59.99	2.18	20.19	$4.57^E -4$	9.24
11	45.35	1.71	17.18	$4.42^E -4$	10.05

**Fig. 4** Effect of alkali concentration on  $\alpha$ -cristobalite (a) and amorphous silica (b) dissolution rate:  $S/L = 2.9/100 \text{ g/g}$ ,  $T = 393.15 \text{ K}$ 

$$\frac{d\alpha}{f(\alpha)} = k(T) dt \quad (1)$$

with  $\alpha$  the conversion rate,  $k(T)$  the rate constant and  $f(\alpha)$  a mathematical function whose equation depends on the mechanism involved.

Integration of Eq. (1) at constant temperature leads to:

$$g(\alpha) = \int_0^\alpha \frac{d\alpha}{f(\alpha)} = k(T) t \quad (2)$$

Using the Arrhenius expression gives:

$$g(\alpha) = A \exp\left(-\frac{E_a}{RT}\right) t \quad (3)$$



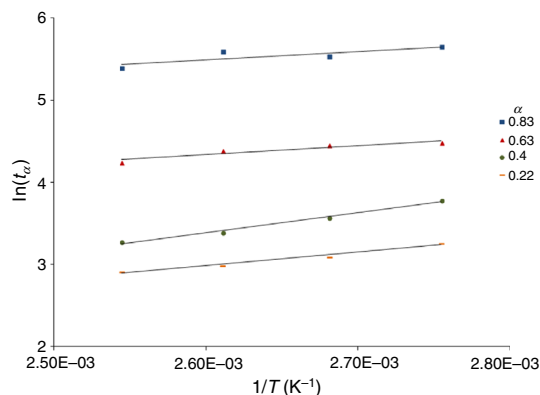


**Fig. 5** Examples of  $\ln(t)$  versus  $1/T$  ( $363.15 \leq T \leq 393.15$  K) for different  $\alpha$  values

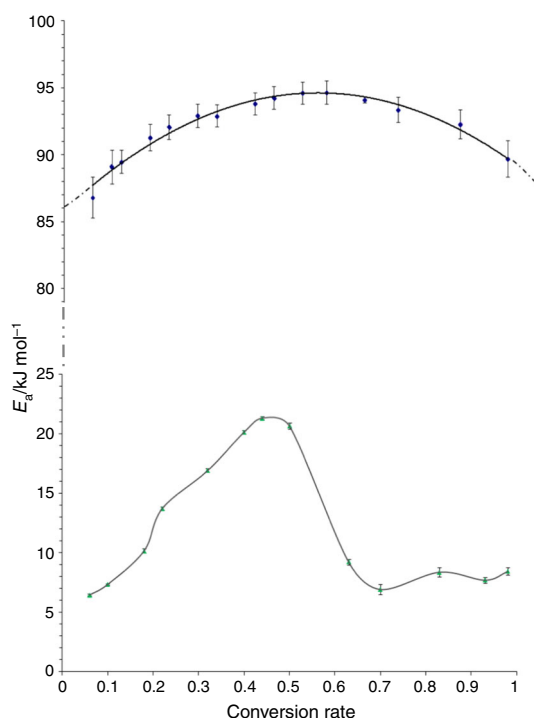


**Fig. 6** Dependence of the activation energy versus the conversion rate, calculated according to the isoconversional model for amorphous silica (triangle) and  $\alpha$ -cristobalite (diamond)

where  $A$  is the pre-exponential factor,  $E_a$  the activation energy and  $R$  the perfect gas constant.

In the shrinking core model,  $E_a$  is constant and the rate is generally controlled by one of the three following steps [21]:

1. Diffusion through the fluid film surrounding the solid particle,
2. Diffusion through the product (ash) layer,
3. Chemical reaction at the surface of unreacted solid.

Integrating the rate equations corresponding to these steps leads to  $g(\alpha)$  as follows:

$$\alpha = kt \text{ (film diffusion control)} \quad (4)$$

$$1 - 3(1 - \alpha)^{2/3} + 2(1 - \alpha) = kt \text{ (ash diffusion control)} \quad (5)$$

$$1 - (1 - \alpha)^{1/3} = kt \text{ (chemical reaction control)} \quad (6)$$

For amorphous silica, the variations in  $g(\alpha)$  with time were plotted for all the experimental data and the linearity has never been observed. Therefore, none of these phenomena is a rate-controlling step. However, the results obtained previously with  $\alpha$ -cristobalite were processed again and showed that dissolution can be roughly described as a chemical-reaction-controlled process with activation energy of  $77.5 \text{ kJ mol}^{-1}$ , which is in the range of values determined in our previous works [9, 10].

### Isoconversional model

This model has been developed many years ago [24–28]. According to it, the change in the mechanism results from the solid surface modification which induced a variation in the activation energy with respect to the conversion rate [29]. Development of this model is based upon expressing Eq (3) as:

$$\ln(t) = \frac{E_a(\alpha)}{RT} + \ln\left(\frac{g(\alpha)}{A}\right) \quad (7)$$

At a certain conversion rate,  $\ln\left(\frac{g(\alpha)}{A}\right)$  is constant, and so, it is possible to determine the activation energy, whatever the mechanism, by plotting  $\ln(t)$  versus  $1/T$  [30]. Calculation was performed for  $\alpha$  in the range 0.06–0.98, and the activation energy was derived. Examples of plots of  $\ln(t)$  versus  $1/T$  ( $363.15 \leq T \leq 393.15$  K) are given in Fig. 5.

The activation energy as a function of  $\alpha$  is represented in Fig. 6 for amorphous silica with the corresponding expanded uncertainties. For the sake of comparison, this quantity is also reminded for  $\alpha$ -cristobalite [9]. The activation energy variation for amorphous silica seems to be more complex.  $E_a$  starts at about  $6 \text{ kJ mol}^{-1}$  and reaches a maximum at  $21 \text{ kJ mol}^{-1}$  for  $\alpha = 0.44$  and then decreases and becomes oscillating around  $8 \text{ kJ mol}^{-1}$  for  $\alpha$  ranging between 0.7 and 1. These values of  $E_a$  correspond to a diffusion-controlled process and not to a chemical-reaction-controlled one as reported in the literature [31–33]. Amorphous state is a metastable one, and so, there should be different forms depending on the manufacturing process and starting materials. Discrepancy with the literature data could result from the difference between the amorphous forms of silica. Nevertheless, the  $E_a$  variation shape



suggests a multi-step process [34] up to  $\alpha = 0.7$  and a one-step process for  $\alpha$  higher than 0.7.

## Conclusions

Microcalorimetry allows highlighting different reactions which cannot be revealed using discontinuous techniques. On the other hand, thermochemical investigations show that oligomers appear successively according to the increase in the formation enthalpy per formula unit. It is commonly stated that, neglecting the entropic contribution, the lower the formation enthalpy of a compound, the higher is its stability and so the earlier it appears. This is true only when comparing compounds having molar masses in the same order of magnitude and not in oligomers series, because the formation enthalpy of a compound depends on the strength and number of the bond energies. This number increases with the molar mass. Finally, kinetic analysis showed that the dissolution process of amorphous silica is more complex than that of  $\alpha$ -cristobalite and cannot be roughly described with a rate-controlling one-step model. Isoconversional model reveals an unusual variation of activation energy over conversion rate.

## References

1. Vannoy WG. Silicate paints. Patent US2449346 A. 1945.
2. Vail JG. Soluble silicates: their properties and uses, vol. 1–2. New York: Reinhold Publishing; 1952.
3. Premakaran TB. Paint comprising water soluble sodium silicate. Patent US5938834 A. 1999.
4. Roggendorf H, Böschel D, Rödicker B. Differential scanning calorimetry at hydrothermal conditions of amorphous materials prepared by drying sodium silicate solutions. *J Therm Anal Calorim*. 2001;63:641–2.
5. Aydin AA, Aydin A. Development of an immobilization process for heavy metal containing galvanic solid wastes by use of sodium silicate and sodium tetraborate. *J Hazard Mater*. 2013;270:35–44.
6. Karami D, Rohani S. Synthesis of pure zeolite Y using soluble silicate, a two-level factorial experimental design. *Chem Eng Process*. 2009;48:1288–92.
7. Eglin D, Shafran KL, Livage J, Coradin T, Perry CC. Comparative study of the influence of several silica precursors on collagen self-assembly and of collagen on 'Si' speciation and condensation. *J Mater Chem*. 2006;16:4220–30.
8. Pawelec KM, Shepherd J, Jugdaohsingh R, Best SM, Cameron RE, Brooks RA. Collagen scaffolds as a tool for understanding the biological effect of silicates. *Mater Lett*. 2015;157:176–9.
9. Fertani-Gmati M, Jemal M. Thermochemistry and kinetics of silica dissolution in NaOH aqueous solution. *Thermochim Acta*. 2011;513:43–8.
10. Fertani-Gmati M, Brahim K, Khattech I, Jemal M. Thermochemistry and kinetics of silica dissolution in NaOH solutions: effect of the alkali concentration. *Thermochim Acta*. 2014;594:58–67.
11. Hill JO, Ojelund G, Wadso I. Thermochemical results for "tris" as a test substance in solution calorimetry. *J Chem Thermodyn*. 1969;1:111–6.
12. Vanderzee CE, Waugh DH, Haas NC, Wigg D. The standard enthalpy of solution of  $\text{NH}_4\text{NO}_3$ (c, IV) in water at 298.15 K. (A search for the standard thermodynamic state.). *J Chem Thermodyn*. 1980;12:27–40.
13. Nichols N, Skold R, Wadso I. Testing of an automatic temperature recording system for an isoperibolic solution calorimeter. *Chem Scr*. 1976;9:110–3.
14. Pattengill MD, Sands DE. Statistical significance of linear-squares parameters. *J Chem Educ*. 1979;56:244–7.
15. Richet P, Bottinga Y, Denielou L, Petitot JP, Tequi C. Thermodynamic properties of quartz, cristobalite and amorphous  $\text{SiO}_2$ : drop calorimetry measurements between 1000 and 1800 K and a review from 0 to 2000 K. *Geochim Cosmochim Acta*. 1982;46:2639–58.
16. <http://www.chem.msu.ru/cgi-bin/tkv.pl>.
17. Gurvich LV, Bergman GA, Gorokhov LN, Iorish VS, Leonidov VYA, Yungman VS. Thermodynamic properties of alkali metal hydroxides. Part 1. Lithium and sodium hydroxides. *J Phys Chem Ref Data*. 1996;25:1211–76.
18. Brahim K, Khattech I, Dubès JP, Jemal M. Etude cinétique et thermodynamique de la dissolution de la fluorapatite dans l'acide phosphorique. *Thermochim Acta*. 2005;436:643–50.
19. Antar K, Brahim K, Jemal M. Etude cinétique et thermodynamique de l'attaque d'une fluorapatite par des mélanges d'acides sulfurique et phosphorique à 25°C. *Thermochim Acta*. 2006;449:35–41.
20. Wen CY. Noncatalytic heterogeneous solid–fluid reaction models. *Ind Eng Chem*. 1968;60:34–54.
21. Levenspiel O. Fluid-particle reactions: kinetics. In: *Chemical Reaction Engineering*. New York: John Wiley; 1972. pp.566–588.
22. Mazet N. Modeling of gas–solid reactions 1. Nonporous solids. *Int Chem Eng*. 1992;32:271–84.
23. Vyazovkin S, Wight CA. Model-free and model-fitting approaches to kinetic analysis of isothermal and nonisothermal data. *Thermochim Acta*. 1999;340–341:53–68.
24. Kissinger HE. Variation of peak temperature with heating rate in differential thermal analysis. *J Res Natl Bur Stand*. 1956;57:217–21.
25. Friedman H. Kinetics of thermal degradation of char-forming plastics from thermogravimetry. Application to a phenolic plastic. *J Polym Sci*. 1964;6C:183–95.
26. Ozawa T. A new method of analyzing thermogravimetric data. *Bull Chem Soc Japan*. 1965;38:1881–6.
27. Flynn JH, Wall LA. General treatment of the thermogravimetry of polymers. *J Res Natl Bur Stand*. 1966;70A:487–523.
28. Akahira T, Sunose T. Joint convention of four electrical institutes. *Res Rep Chiba Inst Technol (Sci Technol)*. 1971;16:22–31.
29. Vyazovkin S, Sbirrazzuoli N. Kinetic methods to study isothermal and nonisothermal epoxy-anhydride cure. *Macromol Chem Phys*. 1999;200:2294–303.
30. Sbirrazzuoli N, Brunel D, Elegant L. Different kinetic equations analysis. *J Therm Anal*. 1992;38:1509–24.
31. Okunev AG, Shaurman SA, Danilyuk AF, Aristov Y, Bergeret G, Renouprez A. Kinetics of the  $\text{SiO}_2$  aerogel dissolution in aqueous NaOH solutions: experiment and model. *J Non-Cryst Solid*. 1999;260:21–30.
32. Niibori Y, Kunita M, Tochiyama O, Chida T. Dissolution rates of amorphous silica in highly alkaline solution. *J Nucl Sci Technol*. 2000;37:349–57.
33. Icenhower JP, Dove PM. The dissolution kinetics of amorphous silica into sodium chloride solutions: effects of temperature and ionic strength. *Geochim Cosmochim Acta*. 2000;64:4193–203.
34. Vyazovkin S. Evaluation of activation energy of thermally stimulated solid-state reactions under arbitrary variation of temperature. *J Comput Chem*. 1997;18:393–402.